OXFORD

GENERAL ARTICLE

Ornithine decarboxylase, the rate-limiting enzyme of polyamine synthesis, modifies brain pathology in a mouse model of tuberous sclerosis complex

David Kapfhamer[1], James McKenna III[1], Caroline J. Yoon[1], Tracy Murray-Stewart[2], Robert A. Casero, Jr[2] and Michael J. Gambello[1,*]

[1]Department of Human Genetics, Emory University School of Medicine, Atlanta, Georgia and [2]The Sidney Kimmel Comprehensive Cancer Center, The Johns Hopkins School of Medicine, Baltimore, MD, USA

*To whom correspondence should be addressed at: 601 Michael Street, Suite 301, Atlanta, GA 30322, USA. Tel: 4047276483; Fax 4047273949; Email: mgambel@emory.edu

Abstract

Tuberous sclerosis complex (TSC) is a rare autosomal dominant neurodevelopmental disorder characterized by variable expressivity. TSC results from inactivating variants within the *TSC1* or *TSC2* genes, leading to constitutive activation of mechanistic target of rapamycin complex 1 signaling. Using a mouse model of TSC (*Tsc2-RG*) in which the *Tsc2* gene is deleted in radial glial precursors and their neuronal and glial descendants, we observed increased ornithine decarboxylase (ODC) enzymatic activity and concentration of its product, putrescine. To test if increased ODC activity and dysregulated polyamine metabolism contribute to the neurodevelopmental defects of *Tsc2-RG* mice, we used pharmacologic and genetic approaches to reduce ODC activity in *Tsc2-RG* mice, followed by histologic assessment of brain development. We observed that decreasing ODC activity and putrescine levels in *Tsc2-RG* mice worsened many of the neurodevelopmental phenotypes, including brain growth and neuronal migration defects, astrogliosis and oxidative stress. These data suggest a protective effect of increased ODC activity and elevated putrescine that modify the phenotype in this developmental *Tsc2-RG* model.

Introduction

The tuberous sclerosis complex (TSC) (OMIM 191100, 613 254) is a rare autosomal dominant disease that often causes substantial central nervous system pathology. Brain phenotypes include cortical tubers, subependymal nodules (SENs), subependymal giant cell astrocytomas (SEGAs) and other morphologic abnormalities. Morbidity and mortality are often due to epilepsy, intellectual disability, autism spectrum disorders and neuropsychiatric disease (1). TSC is caused by inactivating variants in either *TSC1* or *TSC2*, encoding hamartin and tuberin, respectively. These proteins form a complex with TBC1D7 to inhibit the mechanistic

target of rapamycin complex 1 (mTORC1) signaling pathway (2–4). The hyperactivity of mTORC1 signaling due to loss of *TSC1* or *TSC2* induces an anabolic state with an increase in nucleotide, protein, lipid and other macromolecular synthesis to fuel cell growth and proliferation (5). A hallmark of TSC is the intrafamilial and interfamilial variable expressivity among patients. A patient can remain undiagnosed due to relatively benign symptoms, only to be diagnosed after having a severely affected child suffering from recalcitrant epilepsy and developmental delay. While some of the variable expressivity is due to specific pathogenic variants in *TSC1* or *TSC2* (6,7), limited

success has been made in associating disease variability with specific *TSC1* or *TSC2* mutations, degree of mosaicism, genetic modifiers and environmental factors. The identification of novel metabolic targets of mTORC1 hyperactivity may improve our general understanding of TSC biology and its inherent variability.

Using a mouse model of TSC in which the *Tsc2* gene was conditionally targeted in most developing neurons and glial cells of the CNS (*Tsc2-RG*, (8)), we performed untargeted metabolomic profiling studies and found elevated levels of the polyamine putrescine, the product of a rate-limiting enzyme in polyamine synthesis, ornithine decarboxylase (ODC). The activity of ODC was also elevated in the *Tsc2-RG* brains (9), with no change in the downstream polyamine metabolites spermidine or spermine.

Polyamines are small aliphatic polycations with diverse biological functions. Due to their positive charge, polyamines can interact with nucleic acids and proteins and regulate specific ion channels, thereby exerting wide-ranging effects on transcription, translation, RNA and protein stability and cell signaling (10). Polyamine synthesis is a tightly controlled process involving multiple feedback loops, underscoring the biological importance of maintaining proper levels of these metabolites. In eukaryotes, the primary polyamines, putrescine, spermidine and spermine are synthesized mainly from the amino acid ornithine. ODC, a rate-limiting enzyme in polyamine synthesis, converts ornithine to putrescine. Spermidine and spermine are sequentially produced from putrescine by aminopropylation using decarboxylated S-adenosylmethionine (dcSAM) as the aminopropyl donor and catalyzed by spermidine synthase and spermine synthase, respectively (11) (Fig. 1A). dcSAM is the product of the second rate-limiting enzyme in the pathway, S-adenosylmethionine decarboxylase, the processing and stabilization of which is mTORC1-dependent (12). Functionally, polyamines have been shown to play critical roles in cell growth, proliferation and migration; cellular stress; aging; and neurodegenerative diseases (10,13). The observations that (1) *ODC1* is a transcriptional target of proto-oncogene *cMYC* (14), (2) polyamines are involved in cell growth and proliferation and (3) polyamines are upregulated in malignancies have made them a focus of cancer research (15). Currently, multiple clinical studies investigating the therapeutic effects of the irreversible ODC inhibitor 2-difluoromethylornithine (DFMO) on neuroblastoma, astroglioma and other cancers are underway (16–18).

Based on the finding of elevated ODC activity and putrescine levels in *Tsc2-RG* mice, we empirically treated *Tsc2+/−* heterozygous mice with the ODC inhibitor DFMO. *Tsc2+/−* mice have a hippocampal astrogliosis. Amazingly, DFMO treatment dose-dependently reduced hippocampal astrogliosis (9), suggesting a functional consequence of increased ODC/putrescine in TSC pathology. Based on these data, we hypothesized that ODC inhibition and putrescine reduction would similarly improve neurodevelopmental phenotypes of the more severely affected *Tsc2-RG* mice. Using a combination of genetic and pharmacologic approaches, we observed that ODC inhibition and putrescine reduction worsened neuronal growth and migration defects, astrogliosis and oxidative stress in *Tsc2-RG* brains, suggesting a protective effect of elevated putrescine and potentially downstream metabolites in our *Tsc2-RG* model. Moreover, the enzyme ODC is a potent modifier of the TSC brain phenotype. These data establish a role for polyamines in TSC neuropathology and indicate that modulating the polyamine pathway may prove therapeutic for TSC.

Results

Modulation of polyamine synthesis in a mouse model of TSC

Our observation that *Tsc2-RG* mice have increased ODC enzymatic activity in brain prompted us to investigate ODC protein expression in the brains of *Tsc2-RG* mice and TSC patient samples. Although the immunohistochemical (IHC) analysis of ODC expression may not accurately reflect enzymatic activity, we observed qualitatively more ODC immunoreactivity in human TSC tuber giant cells compared with non-tuber control tissue (Fig. 1B and C). These data suggest that elevated ODC may be important in human TSC pathogenesis.

To test our hypothesis that increased ODC activity and putrescine levels in the brains of *Tsc2-RG* mice contribute to TSC neuropathology, we used genetic and pharmacologic approaches to reduce ODC activity in *Tsc2-RG* brains followed by phenotypic analysis (Fig. 2A). The *Tsc2* gene is deleted in radial glial progenitor cells of *Tsc2-RG* mice by Cre-mediated recombination beginning at embryonic day 12.5 (Fig. 2B). In contrast, the *Odc1* gene is expressed much earlier in development with *Odc1−/−* mice dying soon after implantation (19) (Fig. 2B). To genetically reduce ODC activity, we crossed *Tsc2-RG* mice onto an *Odc1+/−* background. *Odc1+/−* mice are viable and fertile despite a 50% reduction in ODC protein and enzyme activity (19,20). Importantly, *Odc1+/−* mice are developmentally normal with none of the neurological phenotypes of *Tsc2-RG* mice. For pharmacologic studies, we reduced ODC activity by treating mice daily from P10 to P21 with intraperitoneal 250 mg/kg DFMO (Fig. 2B). As shown in Figure 2C and D, both treatments reduced ODC activity and putrescine levels, whereas neither treatment altered tuberin levels or mTORC1 activity (Supplementary Material, Fig. S1).

We analyzed experimental mouse brain tissue with ODC immunohistochemistry. While we were unable to quantify ODC antigen, we observed an interesting relocalization of ODC signal. In control cortical and hippocampal pyramidal cells, ODC signal is primarily cytoplasmic (white arrows; Fig. 1D′ and H′). In *Tsc2-RG* mice, the majority of the ODC signal has relocalized to the nucleus (black arrows; Fig. 1E′ and I′). Both pharmacologic and genetic reductions of ODC generated a mixed pattern of nuclear and cytoplasmic staining cells (Fig. 1F′, G′, J′ and K′). Loss of *Tsc2* seems to induce a nuclear rather than cytoplasmic subcellular localization. This localization is reversed with pharmacologic or genetic reduction of *Odc1*.

To try to quantitate how the loss of *Tsc2* and reduction of ODC activity affects *Odc1* regulation, we performed immunoblotting analysis of cortical lysates from control and experimental mice to assess ODC antizyme 1 (OAZ1) expression. OAZ1 participates in a highly complex autoregulatory loop to control polyamine levels, in part by binding to and inactivating ODC and targeting the enzyme for degradation (21). OAZ1 synthesis is stimulated by polyamines via a ribosomal frameshift mechanism and is negatively regulated by antizyme inhibitor protein (22,23). As expected, *Odc1* haploinsufficiency reduced OAZ1 expression compared with control mice, and DFMO treatment almost completely abolished OAZ1 expression in *Tsc2-RG* mice (Supplementary Material, Fig. S2A and B). Unexpectedly, OAZ1 expression was also reduced in the brains of untreated *Tsc2-RG* mice, suggesting that loss of *Tsc2* may induce antizyme inhibitor expression in order to maintain elevated ODC and putrescine levels. A similar reduction in OAZ1 expression has been reported in a *Tsc2*-deficient cell culture model (24).
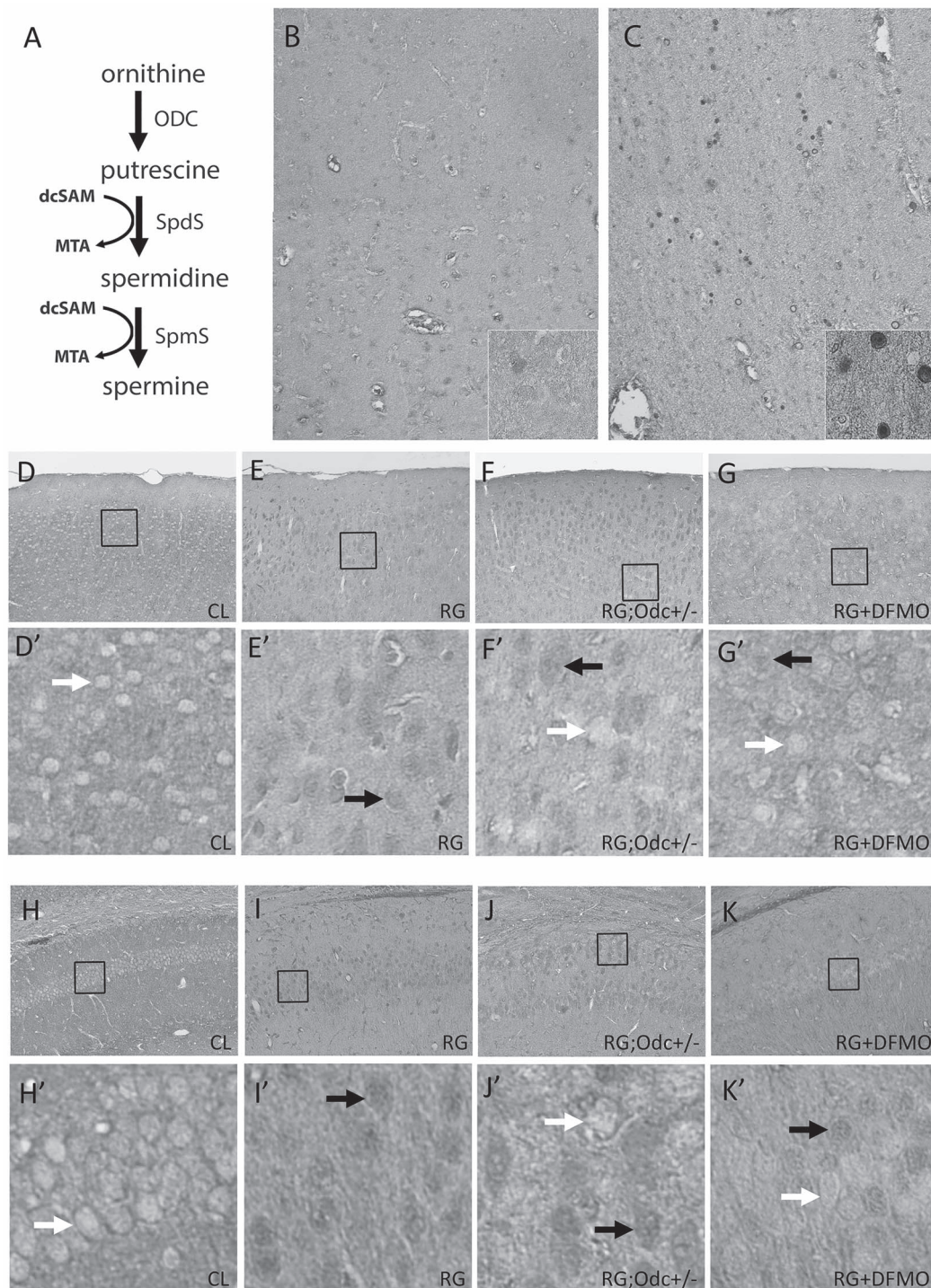
Figure 1. ODC expression in human TSC tuber and mouse *Tsc2-RG* brain. (**A**) Polyamine synthetic pathway. ODC indicates ornithine decarboxylase; SpdS, spermidine synthase; SpmS, spermine synthase; dcSAM, decarboxylated S-adenosylmethionine; MTA, 5′-methylthioadenosine. (**B, C**) IHC analysis showing intense ODC1 staining in giant cells of cortical tuber tissue (C) compared with adjacent cortical non-tuber tissue (B) from a TSC patient. (**D–K, D′–K′**) IHC analysis of ODC1 immunoreactivity in brains of control (D, D′, **H, H′**), untreated *Tsc2-RG* (E, E′, **I, I′**), *Tsc2-RG;Odc1*$^{+/-}$ (F, F′, **J, J′**) and DFMO-treated *Tsc2-RG* (G, G′, K, K′) mice. ODC1 immunoreactivity in cortex (E, E′) and hippocampal CA1 pyramidal cells (I, I′) of untreated *Tsc2-RG* mice and appears localized to both the nucleus and cytoplasm (black arrows), in contrast to control animals (D, D′, H, H′) where expression is primarily cytoplasmic (white arrows). *Odc1* haploinsufficiency and DFMO treatment of *Tsc2-RG* mice partially reverse ODC expression levels and nuclear localization. D′–K′ show increased magnification of boxed inset fields indicated in D–K, respectively. CL indicates control; RG, *Tsc2-RG*; *RG;Odc*$^{+/-}$, *Tsc2-RG;Odc1*$^{+/-}$; RG + DFMO, *Tsc2-RG* + DFMO.
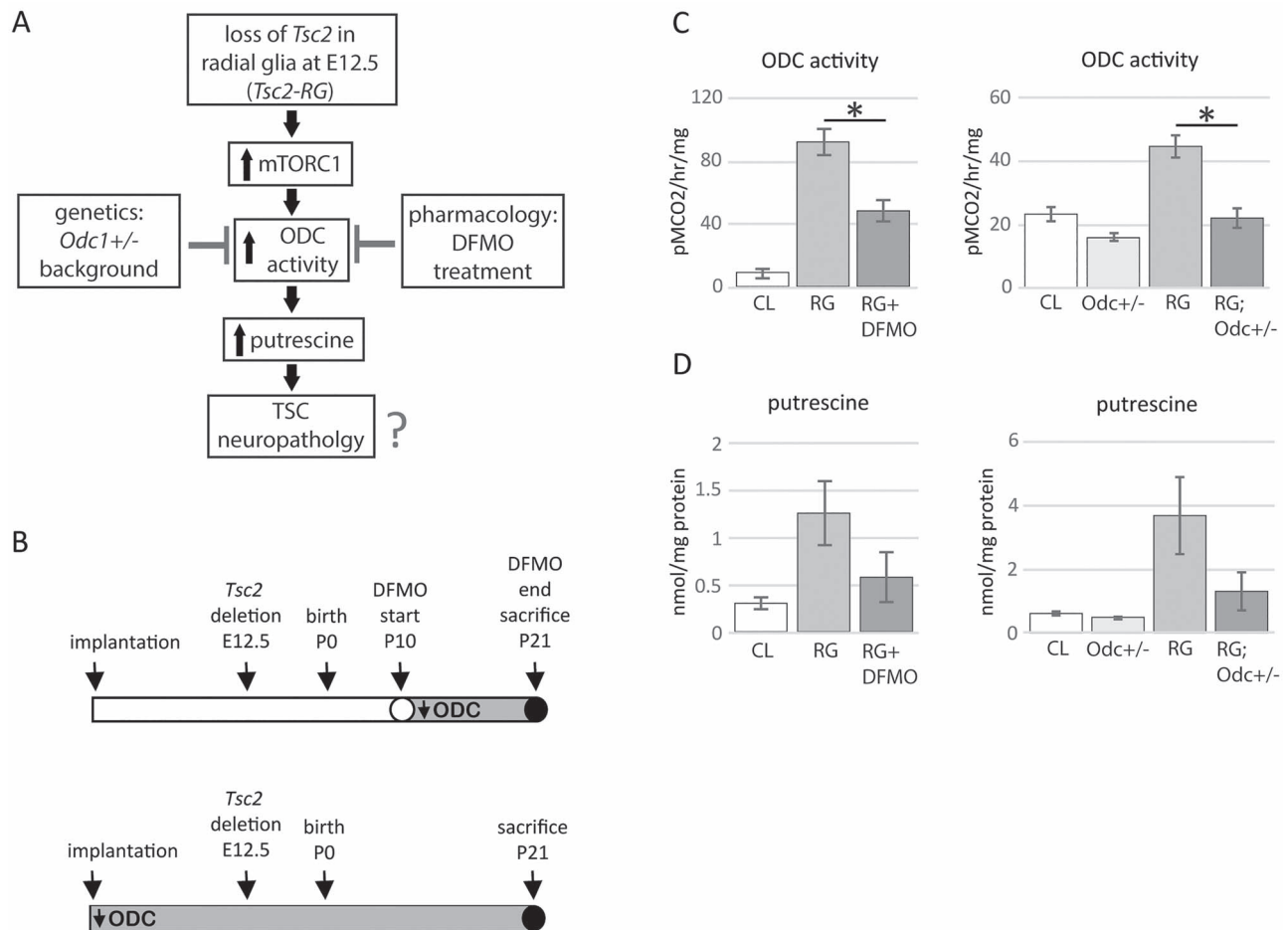
Figure 2. Modulation of polyamine synthesis in a mouse model of TSC. (**A**) *Tsc2* loss in radial glia results in mTORC1 hyperactivation, increased ODC activity and putrescine levels. We investigated the effect on TSC neuropathology following genetic and pharmacologic reduction of ODC. (**B**) Timelines of pharmacologic and genetic reduction of ODC in *Tsc2-RG* mice. Top: DFMO treatment (daily I.P. injection of 250 mg/kg DFMO from P10 to P21) of *Tsc2-RG* mice. Bottom: genetic reduction of *Odc1* beginning prior to implantation. Gray shading of timeline bars denotes period of ODC reduction. (**C, D**) Elevated ODC activity (C) and putrescine levels (D) in *Tsc2-RG* cortex are reduced by DFMO treatment and *Odc1* haploinsufficiency. *$P < 0.05$.

Suppression of polyamine synthesis affects hippocampal and cortical development of *Tsc2-RG* mice

Comparison of the effects of genetic and pharmacologic reduction of ODC on *Tsc2-RG* neuropathology is summarized in Table 1. A common feature of TSC neuropathology is the presence of SENs, which may transform into SEGAs (25,26). We have previously reported that *Tsc2-RG* mice develop ring or nodular heterotopia in the stratum lacunosum moleculare of the hippocampus, and rarely, subependymal-like nodules along the ventricles (8,27). Both lesions develop prior to P10. To investigate the effects of dysregulated polyamine synthesis on hippocampal heterotopia and SENs in *Tsc2-RG* mice, we performed H&E staining of serial brain sections obtained from 21-day-old *Tsc2-RG;Odc1*$^{+/-}$ and control mice. As previously reported, we observed both hippocampal ring heterotopia and subependymal-like nodules in *Tsc2-RG* mice, whereas these were absent in wild-type controls (Fig. 3A, B, E, F). On an *Odc1*$^{+/-}$ background, we observed an increased number of these structures in *Tsc2-RG* mice (Fig. 3C, E and F), indicating that elevated ODC activity and putrescine levels in *Tsc2-RG* mice suppress development of hippocampal heterotopia and SENs.

Tsc2-RG mice are also characterized by increased cortical thickness, a phenotype reminiscent of hemimegalencephaly

Table 1. Phenotypic summary of *Tsc2-RG* mice following genetic or pharmacologic reduction of ODC

Phenotype	*Tsc2-RG; Odc+/−*	*Tsc2-RG* (DFMO)
ODC activity	↓	↓
Putrescine	↓	↓
Hippocampal ring heterotopia	↑	N/A
Subependymal-like nodules	↑	N/A
Cortical thickness	↑	↓
Lamination defects (CUX1)	↑	N/A
Cortical migration defects (BrdU)	↑	N/A
Astrogliosis (GFAP)	↑	↑
Oxidative stress (HO-1)	=	↑
Inflammation (IBA1)	=	=
Hypomyelination (MBP)	=	=

↑ indicates increased; ↓, decreased; =, no change; relative to untreated *Tsc2-RG* mice; N/A, not applicable.

reported in a subset of TSC patients (8,28). H&E staining of brain sections from *Tsc2-RG;Odc1*$^{+/-}$ mice revealed that *Odc1* haploinsufficiency augmented cortical thickness of *Tsc2-RG*
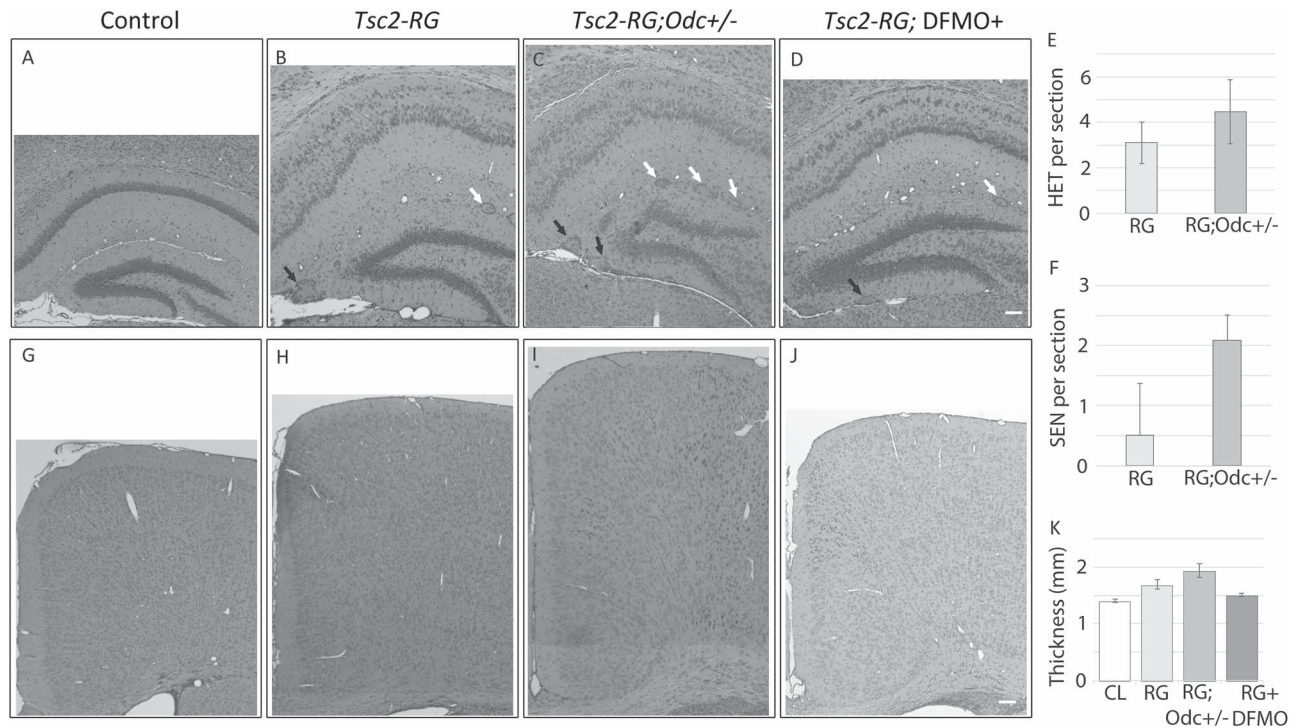
Figure 3. *Odc1* haploinsufficiency increases hippocampal heterotopia (HET), SENs and cortical thickness in *Tsc2-RG* mice. (**A–D**) H&E staining of hippocampi revealed increased number of hippocampal HET and SENs in *Tsc2-RG;Odc1*$^{+/-}$ mice (C) compared with *Tsc2-RG* mice (D). White arrows indicate presence of hippocampal HET; black arrows indicate SENs. HET and SENs are quantified in (**E**) and (**F**), respectively. (**G–J**) H&E staining of cortex shows increased cortical thickness in *Tsc2-RG;Odc1*$^{+/-}$ mice (I) compared with *Tsc2-RG* mice (H). Cortical thickness is quantified in panel (**K**).

mice (Fig. 3G–I and K). Surprisingly, DFMO treatment of *Tsc2-RG* mice from P10 to 21 had the opposite effect, with cortical thickness of treated *Tsc2-RG* mice comparable with that of wild-type control animals (Fig. 3G, J and K). These data indicate a complex effect of polyamines on cortical development.

Cortical lamination and neuronal migration defects in *Tsc2-RG* mice are more severe on an *Odc1*$^{+/-}$ background

Another neurodevelopmental phenotype of *Tsc2-RG* mice is the presence of cortical lamination defects due to abnormal neuronal migration (8). Polyamines have been implicated in cell proliferation and migration (13), prompting us to investigate if the cortical organization phenotypes in *Tsc2-RG* mice are modified by ODC inhibition and polyamine depletion. These phenotypes in *Tsc2-RG* mice develop prior to postnatal day 10, the onset of DFMO treatment in our pharmacologic study; therefore, we focused on the effect of constitutive *Odc1* haploinsufficiency on cortical organization. The transcription factor CUX1, expressed primarily in cortical layers II–IV (29), was used to assess lamination defects. By IHC analysis, a significantly higher percentage of CUX1-positive ectopic cells (layers V and VI) were observed in *Tsc2-RG* than control cortex, as previously reported (8). Compared with *Tsc2-RG* brains, *Tsc2-RG;Odc1*$^{+/-}$ brains showed an additional increase in the percentage of ectopic CUX1-positive cells (Fig. 4A–D and I). We next performed BrdU pulse-labeling of cortical neurons at E15.5. Most neurons labeled at E15.5 will eventually migrate to the upper layers of the cerebral cortex. We found no significant difference in the total number or distribution of BrdU-labeled cells between control and *Odc1*$^{+/-}$ mice (Fig. 4E, F and J). As previously reported, we observed more

labeled cells closer to the ventricular zone (bins 5) in *Tsc2-RG* mice, supporting a role for tuberin in neuronal migration (Fig. 4E, G and J). Even more BrdU-labeled neurons were observed in bin 5 in the cortex of *Tsc2-RG;Odc1*$^{+/-}$ mice (Fig. 4E–H and J). Thus, *Odc1* haploinsufficiency exacerbates the neuronal migration defects due to loss of *Tsc2*. These results suggest that ODC activity is an important modifier of cortical lamination in a *Tsc2*-deficient background.

Genetic and pharmacologic reduction of ODC activity increases reactive astrogliosis in the cortex of *Tsc2-RG* mice

Our previous finding that DFMO treatment dose-dependently reduced hippocampal astrogliosis in *Tsc2*$^{+/-}$ mice suggested that DFMO and/or *Odc1* haploinsufficiency may have a similar effect on reducing hippocampal and cortical astrogliosis in *Tsc2-RG* mice. To our surprise, we observed a dramatic increase in GFAP immunofluorescence in the brains of both *Tsc2-RG;Odc1*$^{+/-}$ and DFMO-treated *Tsc2-RG* mice compared with untreated *Tsc2-RG* controls (Fig. 5A–D and I). These data indicate that elevated ODC activity and putrescine levels in *Tsc2-RG* mice ameliorate some of the reactive astrogliosis triggered by loss of *Tsc2*.

DFMO treatment of *Tsc2-RG* mice increases cortical oxidative stress

Earlier work established a function of polyamines in protection against oxidative stress, in part by acting directly as free radical scavengers (30). To determine if the increased astrogliosis we
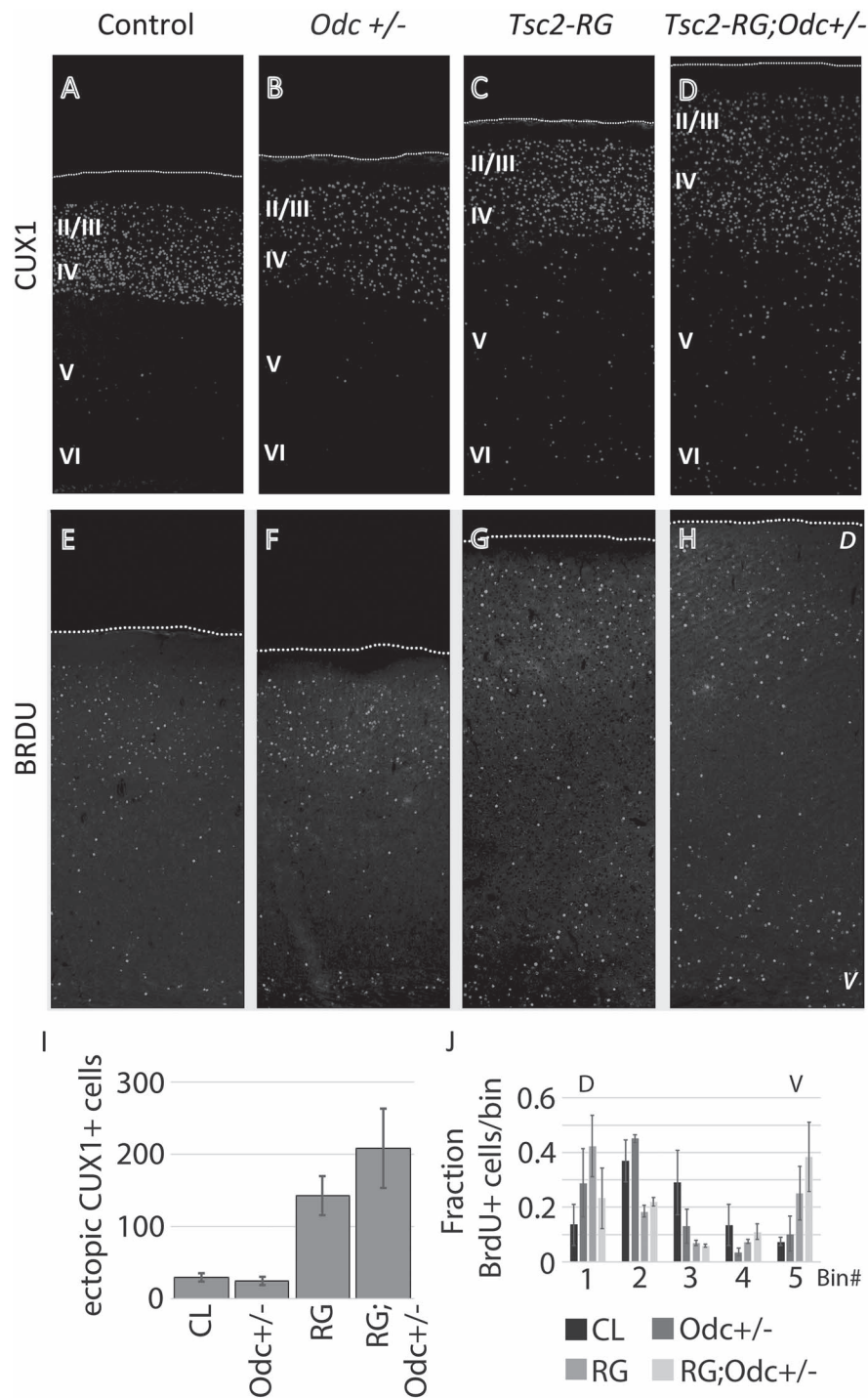
Figure 4. Cortical lamination and neuronal migration defects in *Tsc2-RG* mice are more severe on an *Odc1*$^{+/-}$ background. (**A–D, I**) CUX1 immunofluorescence in cortex of P21 mice. CUX1 labels neurons primarily in cortical layers II–IV as indicated in control mouse (**A**). Ectopically labeled cells in deeper cortical layers are increased in *Tsc2-RG* and *Tsc2-RG;Odc1*$^{+/-}$ mice (C, D, I). Cortical layers are indicated with Roman numerals. (**E–H, J**) BrdU pulse-labeling of cortical neurons on E15.5 reveals neuronal migration defects in *Tsc2-RG* and *Tsc2-RG;Odc1*$^{+/-}$ mice. Cortices were subdivided in five bins of equal thickness (bin #1 most dorsal) and fractions of BrdU-positive cells per bin were calculated. *Tsc2-RG* and *Tsc2-Odc1*$^{+/-}$ brains had a higher fraction of BrdU-positive cells in the ventral-most area. *D* indicates dorsal; *V* ventral.

observed in *Tsc2-RG;Odc1*$^{+/-}$ and DFMO-treated *Tsc2-RG* brains is associated with increased oxidative stress, we performed immunofluorescence experiments using anti-heme oxygenase 1 (HO-1) antibody. HO-1 catalyzes the degradation of heme to biliverdin, ferrous iron and carbon monoxide, and its expression is induced by oxidative stress (31). We observed increased HO-1 immunoreactivity in the brains of *Tsc2-RG* mice compared with control animals, consistent with previous
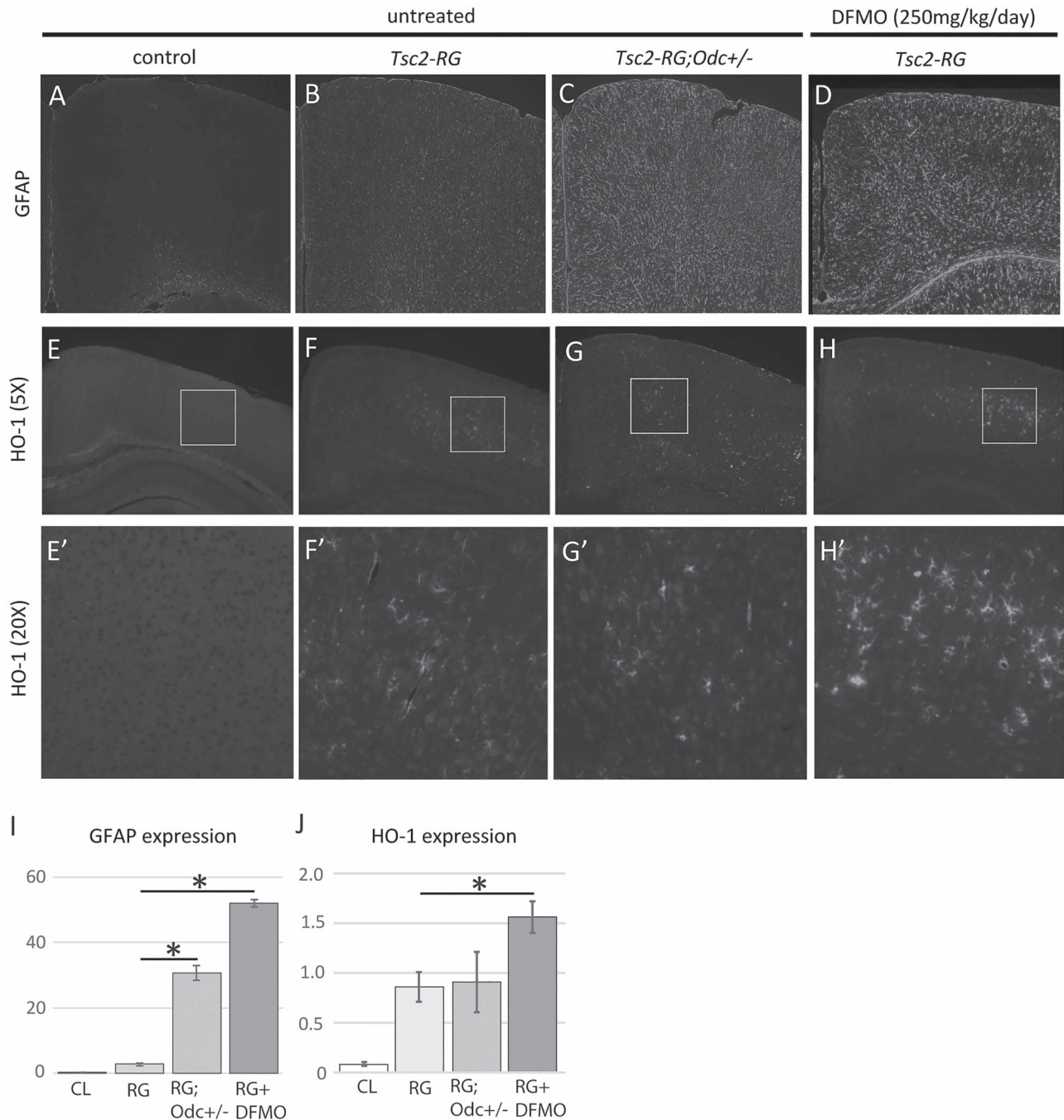
Figure 5. Genetic and pharmacologic reduction of ODC activity increases cortical astrogliosis and oxidative stress in *Tsc2-RG* mice. (**A–D**) GFAP immunofluorescence showing increased labeling of astrocytes throughout the cortex of *Tsc2-RG* mice (B) compared with control animals (A). GFAP signal in *Tsc2-RG* mice is further increased on an $Odc1^{+/-}$ background (C) or following DFMO treatment (D). (**E–H, E′–H′**) HO-1 immunofluorescence showing increased reactivity in *Tsc2-RG* (F, F′) cortex compared with control mice (E, E′). HO-1 is a marker of oxidative stress. Treatment of *Tsc2-RG* mice with DFMO (H, H′) further increased HO-1 staining, whereas *Odc1* haploinsufficiency had no effect (G, G′). E′–H′ show increased magnification of boxed inset fields indicated in E–H, respectively. (**I, J**) Quantification of immunoreactivity for GFAP (I) and HO-1 (J).

studies (32–34), and a further increase in HO-1 immunoreactivity upon DFMO treatment of *Tsc2-RG* mice. HO-1 expression appeared unchanged in *Tsc2-RG* mice on an $Odc1^{+/-}$ background (Fig. 5E–H, E′–H′ and J). Colocalization of HO-1 and vimentin, an astrocytic marker, confirmed that the increased HO-1 expression was primarily restricted to astrocytes (Supplementary Material, Fig. S3), indicating that the ODC inhibition in *Tsc2-RG* mice increases oxidative stress within astrocytes.

Reduction of ODC activity does not affect neuroinflammation or myelination in *Tsc2-RG* mice

Microglia, the resident immune cells within the CNS, are reported to infiltrate cortical tubers and SEGAs from TSC patients and are increased in the brains of other TSC mouse models (35–37). Furthermore, polyamines may exert anti-inflammatory effects (38), suggesting that ODC inhibition may

increase inflammation in the brains of *Tsc2-RG* mice. To test this possibility, we performed immunofluorescence of control, *Tsc2-RG*, *Tsc2-RG;Odc1*$^{+/−}$ and DFMO-treated *Tsc2-RG* brains using an anti-IBA1 antibody, a marker of microglia and macrophages. Consistent with previous work, IBA1 brain immunoreactivity was markedly increased in *Tsc2-RG* mice (Supplementary Material, Fig. S4), indicating an inflammatory response. Reduction of ODC activity, either genetically or pharmacologically, did not appear to affect IBA1 immunoreactivity (Supplementary Material, Fig. S4) in *Tsc2-RG* brains. Although we did not directly assess the expression of specific pro- or anti-inflammatory genes in our model, our data suggest that ODC inhibition has little or no effect on neuroinflammation in *Tsc2-RG* mice.

Hypomyelination has been described as a clinical feature of human TSC lesions and has been observed in mouse models of TSC (8,39–41). To assess the effects of ODC reduction on hypomyelination in *Tsc2-RG* mice, we performed immunofluorescence of control, *Tsc2-RG*, *Tsc2-RG;Odc1*$^{+/−}$ and DFMO-treated *Tsc2-RG* brains using an anti-MBP antibody, a marker of myelin basic protein. As previously reported, we observed decreased MBP immunoreactivity in *Tsc2-RG* brain compared with controls (Supplementary Material, Fig. S5A and B). Neither genetic nor pharmacologic reduction of ODC activity appeared to affect MBP staining in *Tsc2-RG* mice (Supplementary Material, Fig. S5C and D), indicating that ODC inhibition does not grossly alter myelination
in our model.

Discussion

Using complementary genetic and pharmacologic means, we reduced cortical ODC activity and putrescine in *Tsc2-RG* mice to comparable levels without affecting spermine or spermidine. While we did observe differences in resulting phenotypes (Table 1), the general outcome was a worsening of TSC-related pathology. These data support the hypothesis that elevated putrescine and/or its derivatives are a protective mechanism to counteract multiple mTORC1-induced neurodevelopmental defects in *Tsc2-RG* mice. Recently, dysregulated polyamine metabolism has also been reported upon rapalog treatment of lymphangioleiomyomatosis, a TSC-associated cystic lung disease, implicating polyamines in TSC pathogenesis of multiple organ systems (42).

Gain-of-function *ODC1* mutations have been identified in humans, resulting in macrocephaly, white matter abnormalities, developmental delay and additional phenotypes (43,44). In contrast, overexpression of *Odc1* in mice does not appear to affect normal, gross brain morphology (45,46), underscoring fundamental differences in ODC and polyamine function in brain development between humans and mice. Interestingly, *Odc1* overexpressing mice are resistant to chemically and electrically induced seizures (46), indicating that increased putrescine and its derivatives may be protective for TSC-related epilepsy. Apart from the general effects of polyamines on transcription and translation, studies suggest that polyamines may exert anticonvulsant effects via conversion of putrescine to GABA (47,48) and inhibition of voltage-gated sodium channels (49). Although we did not directly assess epileptiform/seizure activity in the present study, we observed that *Tsc2-RG;Odc1*$^{+/−}$ and DFMO-treated *Tsc2-RG* mice die earlier than *Tsc2-RG* mice, suggesting that seizure activity may be enhanced by ODC inhibition in our model.

Cortical lamination, HC heterotopia, SENs and cortical thickness

ODC and polyamines play a role in the aberrant cortical development resulting from *Tsc2* deletion. Prenatal reduction of ODC in *Tsc2-RG; Odc1*$^{+/−}$ mice resulted in an increased number of ectopic neurons in deep cortical layers, indicative of a worsened cortical lamination defect. We also observed an increased incidence of hippocampal heterotopia in *Tsc2-RG* mice on an *Odc1*$^{+/−}$ background. We did not analyze these lesions in the DFMO-treated mice as these defects have been shown to occur before P10 when DFMO administration was started in the pharmacologic group (8,27). We tried to treat animals with DFMO starting from birth, but the dose used made the animals extremely sick, underscoring the importance of ODC1 during cell growth and proliferation. Although the functional significance of these lesions is unclear, it has been hypothesized that they may result from abnormal migration of neural stem cells from the subventricular zone (SVZ) (8). One major clinical feature of TSC that has been inconsistently recapitulated in mouse models is the development of periventricular nodular lesions, or SENs. SENs are present in 80–90% of TSC patients and are considered precursors of SEGAs. We and other investigators have reported the presence of SEN-like lesions in *Tsc1*-deficient mice, and less frequently, in *Tsc2-RG* mice (27,50,51). In the present study, we consistently observed SENs in *Tsc2-RG;Odc1*$^{+/−}$ mice (4/4 animals), representing a reliable model for future studies of SEN development. Like hippocampal heterotopia, it has been proposed that SENs result from abnormal migration of neural stem/progenitor cells within the SVZ (50). These observations suggest that dysregulated polyamine-dependent expression of cell migration/guidance cues in the CNS may underlie these malformations of cortical development.

We did observe reduced cortical thickness in the DFMO-treated mice. DFMO is a potent inhibitor of cell proliferation (16). We administered DFMO from P10 to P21, timing that precludes cell fate perturbations. Nonetheless, DFMO could have inhibited glial proliferation leading to the reduced cortical thickness we observed in DFMO-treated animals compared with *Tsc2-RG;Odc1*+/− animals. DFMO can also inhibit arginase affecting the flow of nitrogen through the urea cycle and the flux of ornithine (52). This off-target effect may also explain the difference in cortical thickness observed. Lastly, DFMO is a suicide substrate, binding irreversibly to ODC1 after decarboxylation. The dead enzyme might exert some unknown toxic effects. Both DFMO treatment and *Odc1* haploinsufficiency worsened reactive astrogliosis, though astrogliosis was associated with increased oxidative stress only in DFMO-treated mice.

Astrogliosis

One of the most striking and unexpected results of this study was the observation that ODC inhibition dramatically increased reactive astrogliosis in *Tsc2-RG* mice. We have previously shown that DFMO dose-dependently reduced hippocampal astrogliosis in *Tsc2*$^{+/−}$ mice. Why ODC inhibition has opposite effects in these two models is unclear. In experiments using cultured astrocytes, we observed that DFMO inhibited mTORC1 signaling in *Tsc2*$^{+/+}$ and *Tsc2*$^{+/−}$ but not *Tsc2*$^{−/−}$ cells (Supplementary Material, Fig. S1). However, we failed to detect an effect of DFMO on mTORC1 signaling *in vivo* in *Tsc2*$^{+/−}$ or *Tsc2-RG* mice (Supplementary Material, Fig. S1), perhaps due to sampling mixed cell populations (whole cortex), *in vivo* drug bioavailability/turnover

or some unidentified reason. Previous studies have shown regulation of ODC expression by mTORC1 activity (53,54); however, to our knowledge, a feedback mechanism has not been described. This apparent *Tsc2*-dependent negative feedback of DFMO on mTORC1 activity in culture might underlie the seemingly contradictory effects of DFMO on astrogliosis in *Tsc2*$^{+/-}$ and *Tsc2-RG* mice, and if confirmed, could be useful in differentially targeting *Tsc2*-expressing versus *Tsc2* null cells.

Similar to *Tsc2-RG* mice (8), other TSC mouse models (9,27,55–57), cell culture models in which the *Tsc1* or *Tsc2* genes have been deleted (58–60), and tubers from TSC patients (61) exhibit an increase in astrocyte number. It has been proposed that TSC1/2 loss causes a shift in cell fate from neurons to astrocytes (59). Our data suggest that this cell fate specification may be further modulated by polyamines. Additionally, reactive astrogliosis may result from seizure activity or other insults (62), consistent with the hypothesis that elevated putrescine/derivatives in *Tsc2-RG* mice may have anticonvulsant effects.

Increased oxidative stress

We also observed that DFMO increased HO-1expression in *Tsc2-RG* cortex, primarily within astrocytes. *Hmox1* is upregulated in response to oxidative stress, converting heme to the antioxidants bilirubin and biliverdin, thus exerting a protective effect (31). Additionally, this degradation of heme generates carbon monoxide and iron, which may exacerbate cellular stress under chronically upregulated HO-1 conditions. Thus, the consequences of increased HO-1 expression are complex and have been associated with neurodegeneration in Parkinson's and Alzheimer's diseases (63,64). In epilepsy models, an increase in HO-1 expression post-seizure has been associated with overexpression of the upstream transcription factor, nuclear factor erythroid 2-related factor 2 (*Nrf2*) (65). RNAseq analysis of *Tsc2-RG* cortical tissue similarly shows increased expression of both *Nrf2* and *Hmox1* (data in preparation). Observations that polyamines act as free radical scavengers (66,67) are consistent with the increased oxidative stress and HO-1 expression in *Tsc2-RG* brains upon ODC inhibition/putrescine depletion.

ODC1 cellular localization

One surprising observation in our study is the apparent enrichment of nuclear ODC1 protein in *Tsc2-RG* cortex and hippocampus and partial reversal by DFMO treatment or *Odc1* haploinsufficiency. Within the hippocampal CA1 pyramidal layer of control mice we observed primarily cytoplasmic ODC1 immunoreactivity, consistent with previous work (46,68). In these studies, neither ODC1 overexpression nor ischemia grossly altered ODC1 subcellular localization, suggesting that the changes we observe in *Tsc2-RG* mice may be TSC and/or seizure-specific. The functional implications of these changes in ODC1 subcellular localization are unclear. Factors affecting the ratio of nuclear to cystosolic ODC1 include cell type, cell cycle, disease state and other physiologic factors, with the caveat that the methodology used to measure ODC1 may confound the results (69,70). In the present study, we used immunohistochemical analysis, which may not differentiate between active and inactive ODC1 enzyme, complicating interpretation of the data. In cell fractionation studies, it has been reported that nuclear ODC1 in multiple brain regions is more likely to be enzymatically active than cytoplasmic ODC1, resulting in increased nuclear putrescine (71). One might postulate that altering nuclear ODC1/putrescine may directly impact gene transcription and RNA processing/stability;

however, additional work will be required to determine the functional consequences of increased nuclear ODC1 in *Tsc2-RG* mice and associated neuropathology.

In conclusion, we report that reduction of ODC activity and downstream polyamine metabolism modifies many of the neurodevelopmental phenotypes in a mouse model of TSC. Differential ODC activity may contribute to the variable disease severity of TSC patients. These data underscore the functional significance of polyamines in regulating neuronal migration, reactive astrogliosis and oxidative stress and define a biological pathway that may be targeted by pharmacologic and/or dietary means to improve TSC disease outcome. To this end, future studies will focus on *increasing* ODC activity/putrescine production as a means to improve neurodevelopmental phenotypes in *Tsc2-RG* mice, as well as investigating whether modifying polyamine metabolism might affect post-developmental defects associated with TSC.

Materials and Methods

Animals and drug treatment

All animal experiments were approved by the Emory University Institutional Animal Care and Use Committee and were carried out in accordance with the Guide for the Humane Use and Care of Laboratory Animals. We generated and genotyped *Tsc2-RG* mice (*Tsc2*$^{flox/-}$; *hGFAP-Cre*) and controls (*Tsc2*$^{flox/+}$) as previously described (8). To generate *Tsc2-RG;Odc1*$^{+/-}$ and control mice, we crossed *Odc1*$^{+/-}$; *Tsc2*$^{+/-}$; *hGFAP-Cre* X *Tsc2*$^{flox/flox}$ mice. Mice were genotyped for *Odc1*-deleted and wild-type alleles by multiplexing three primers in one PCR: Odc35: 5′-CTCTGTAAGTACGGGAAGCCC-3′, Odc43: 5′-CGAGGTCCGCAACATAGAACG-3′ and OdcNeo: 5′-CCCACACCTCC CCCTGAACC-3′. Band sizes were 270 bp for wild-type and 470 bp for knockout alleles. *Odc1*$^{+/-}$ mice were a generous gift from Dr John Cleveland, Moffitt Cancer Center. For DFMO experiments, mice were treated intra-peritoneally with a single daily dose of 250 mg/kg DFMO diluted in sterile PBS, from P10 to P21. DFMO was a generous gift from Dr Patrick M. Woster, MUSC. Using timed matings, pregnant dams were injected at E15.5 with 50 mg/kg BrdU, ip, dissolved in 7 mM NaOH/PBS.

ODC activity and determination of intracellular polyamines

Tissue homogenates were prepared on ice using a tissue tearor in buffer containing 25 mM TrisCl, pH 7.5, 0.1 mM EDTA and 2.5 mM DTT. ODC activity was measured as the release of radiolabeled CO_2 following incubation with [^{14}C]-ornithine, as previously described (72). Aliquots of these lysates were also used for acid extraction and precolumn dansylation followed by HPLC analysis to determine intracellular concentrations of the individual polyamines (73). Both ODC activity and polyamine concentration are presented relative to total cellular protein, which was measured by the method of Bradford using interpolation on a bovine serum albumin standard curve (74).

Human tissue samples

Human tissue was obtained from the NICHD Brain and Tissue Bank for Developmental Disorders at the University of Maryland, Baltimore, MD. The NICHD Brain and Tissue Bank fixed the right side of the patient's brain in 10% formalin. The tuber sample and control sample were from the same TSC patient, a 56-year-old female. In addition to TSC, she had diffused interstitial

lung disease. Her medications were valsartan, hydrochlorothiazide, prednisone, vitamin D, calcium, moxifloxacin, inhaled tiotropium, ipratropium and albuterol.

Primary astrocyte cultures

Neocortical astrocyte cultures were generated from individual P0-2 mice as described previously (75) and genotyped. Purity of cultures was assessed by immunofluorescence using astrocyte-specific markers with anti-GFAP and anti-vimentin antibodies (see below). Experiments were performed at passages 2–4. Briefly, astrocytes were seeded in 9.6 cm^2 wells and grown to 75% confluence. On the day of treatment, growth medium [DMEM/F12 (1:1), 10% fetal bovine serum, 4.6 g/L glucose, 50 μg/ml penicillin, 50 μg/ml streptomycin] was removed and replaced with fresh medium with or without DFMO (15 mM) for 2 h. Following treatment, cells were washed with PBS and trypsinized and protein was extracted for immunoblotting. Experiments were performed in triplicate.

Protein analysis

Antibodies used for western blot analysis were as follows: mouse anti-β-actin and mouse anti-GFAP (1:2000, Sigma-Aldrich, St. Louis, MO), rabbit anti-tuberin, total rabbit anti-S6, phosphorylated (S240/244) rabbit anti-S6 and rabbit anti-α-tubulin (1:1000, Cell Signaling Technology, Bedford, MA), mouse anti-HO-1 (1:1000, Enzo Life Sciences, Farmingdale, NY), rabbit anti-IBA1 (1:1000, Fujifilm Wako Pure Chemical Corp., Osaka, Japan) and rabbit anti-OAZ1 (1:2000, a generous gift from Dr Senya Matsufuji at The Jikei University School of Medicine, Minato-ku, Japan). Experiments were performed with a minimum of three biological replicates. Whole cell lysates were made from day P21 cerebral cortex that was quick-frozen in liquid nitrogen. Samples were homogenized in a Dounce homogenizer with 10 volumes of RIPA buffer with protease inhibitor cocktail and phosphatase inhibitor cocktail (Sigma-Aldrich). Lysates were centrifuged at 4°C, sonicated and frozen until use. Protein concentrations were determined with a Pierce BCA reagent kit (ThermoFisher Scientific, Rockford, IL). Equal amounts of protein were separated on a denaturing 4–12% gradient gel (Invitrogen, Carlsbad, CA) and transferred to PVDF membranes (Immobilon, Sigma-Aldrich). Secondary antibodies were horseradish peroxidase-conjugated. Visualization was conducted with an ECL kit (Amersham, Piscataway, NJ, USA) and a ChemiDoc™ Imaging System (Bio-Rad, Hercules, CA). Protein band intensities were quantified with ImageJ software and normalized to β-actin or α-tubulin control bands.

Histology

Histological analysis was performed with a minimum of three animals per experimental group. P21 mice were deeply anesthetized before undergoing transcardiac perfusion with PBS followed by 4% paraformaldehyde (PFA). Mouse brains were post-fixed in PFA overnight and stored in 70% ethanol prior to embedding in paraffin. Paraffin blocks were sectioned at 8 μm and slide-mounted. Slides were rehydrated, stained with routine H&E and coverslipped. For DAB immunohistochemistry, slides were incubated with 0.3% H_2O_2 in methanol for 20 min before the application of primary antibody [rabbit anti-ODC1 (1:100, Proteintech Group Inc., Rosemont, IL)]. After biotinylated secondary antibody incubation, the slides were washed and incubated in Vectastain ABC working solution (Vector Laboratories, Burlingame, CA). DAB (Cell Signaling, #8059) was

used for visualization. Immunofluorescence was performed as previously described (8) using mouse anti-GFAP antibody (1:400, Sigma-Aldrich), rabbit anti-CUX1 (1:50, Santa Cruz Biotechnology, Santa Cruz, CA), mouse anti-HO-1 (1:100, Enzo Life Sciences), rabbit anti-IBA1 (Fujifilm Wako Pure Chemical Corp.), rabbit anti-vimentin (1:200, Cell Signaling Technology) and anti-BrdU (1:50, Becton Dickinson). Secondary antibodies (1:250; Invitrogen) were Alexa Fluor 488 (anti-rabbit IgG) (anti-mouse IgG$_1$) and Alexa Fluor 555 (anti-rabbit IgG) (anti-mouse IgG$_1$) (anti-mouse IgG$_{2a}$). Tissue images were examined using a Leica DM6000 and captured with a QImaging RETIGA-2000RV digital camera. Digital images were then processed using Adobe Photoshop CS6 (San Jose, CA, USA). Quantification of immunofluorescence was performed using ImageJ software by calculating the number of pixels above the intensity of background signal determined for each subject and expressed as a percentage of total pixels in the field of analysis.

Supplementary Material

Supplementary Material is available at *HMG* online.

References

1. Crino, P., Nathanson, K. and Henske, E. (2006) The tuberous sclerosis complex. *N. Engl. J. Med.*, **355**, 1345–1356.
2. European Chromosome 16 Tuberous Sclerosis Consortium (1993) Identification and characterization of the tuberous sclerosis gene on chromosome 16. *Cell*, **75**, 1305–1315.
3. van Slegtenhorst, M., de Hoogt, R., Hermans, C., Nellist, M., Janssen, B., Verhoef, S., Lindhout, D., van den Ouweland, A., Halley, D., Youngal, J. *et al.* (1997) Identification of the tuberous sclerosis gene TSC1 on chromosome 9q34. *Science*, **277**, 805–808.
4. Dibble, C., Elis, W., Menon, S., Qin, W., Klekota, J., Asara, J., Finan, P., Kwiatkowski, D., Murphy, L. and Manning, B.D. (2012) TBC1D7 is a third subunit of the TSC1-TSC2 complex upstream of mTORC1. *Mol. Cell*, **47**, 535–546.
5. Ben-Sahra, I. and Manning, B.D. (2017) mTORC1 signaling and the metabolic control of cell growth. *Curr. Opin. Cell Biol.*, **45**, 72–82.
6. Kozlowski, P., Roberts, P., Dabora, S., Franz, D., Bissler, J., Northrup, H., Au, K.S., Lazarus, R., Domanska-Pakiela, D.,

Kotulska, K. *et al.* (2007) Identification of 54 large deletions/duplications in TSC1 and TSC2 using MLPA, and genotype-phenotype correlations. *Hum. Genet.*, **121**, 389–400.

7. Peron, A., Au, K.S. and Northrup, H. (2018) Genetics, genomics, and genotype-phenotype correlations of TSC: insights for clinical practice. *Am. J. Med. Genet. C Semin. Med. Genet.*, **178**, 281–290.

8. Way, S., McKenna, J., III, Mietzsch, U., Reith, R., Wu, H. and Gambello, M. (2009) Loss of Tsc2 in radial glia models the brain pathology of tuberous sclerosis complex in the mouse. *Hum. Mol. Genet.*, **18**, 1252–1265.

9. McKenna, J., III, Kapfhamer, D., Kinchen, J.M., Wasek, B., Dunworth, M., Murray-Stewart, T., Bottiglieri, T., Casero, R.A.J. and Gambello, M.J. (2018) Metabolomic studies identify changes in transmethylation and polyamine metabolism in a brain-specific mouse model of tuberous sclerosis complex. *Hum. Mol. Genet.*, **27**, 2113–2124.

10. Miller-Fleming, L., Olin-Sandoval, V., Campbell, K. and Raiser, M. (2015) Remaining mysteries of molecular biology: the role of polyamines in the cell. *J. Mol. Biol.*, **427**, 3389–3406.

11. Ikeguchi, Y., Bewley, M.C. and Pegg, A.E. (2006) Aminopropyltransferases: function, structure and genetics. *J. Biochem.*, **139**, 1–9.

12. Zabala-Letona, A., Arruabarrena-Aristorena, A., Martin-Martin, N., Fernandez-Ruiz, S., Sutherland, J.D., Clasquin, M., Tomas-Cortazar, J., Jimenez, J., Torres, I., Quang, P. *et al.* (2017) mTORC1-dependent AMD1 regulation sustains polyamine metabolism in prostate cancer. *Nature*, **547**, 109–113.

13. McCormack, S.A. and Johnson, L.R. (2001) Polyamines and cell migration. *J. Physiol. Pharmacol.*, **52**, 327–349.

14. Bello-Fernandez, C., Packham, G. and Cleveland, J.L. (1993) The ornithine decarboxylase gene is a transcriptional target of c-Myc. *Proc. Natl. Acad. Sci. U. S. A.*, **90**, 7804–7808.

15. Casero, R.A.J., Murray Stewart, T. and Pegg, A.E. (2018) Polyamine metabolism and cancer: treatments, challenges and opportunities. *Nat. Rev. Cancer*, **18**, 681–695.

16. LoGiudice, N., Le, L., Abuan, I., Leizorek, Y. and Roberts, S.C. (2018) Alpha-difluoromethylornithine, an irreversible inhibitor of polyamine biosynthesis, as a therapeutic strategy against hyperproliferative and infectious diseases. *Med. Sci.*, **6**, E12.

17. Alexiou, G.A., Lianos, G.D., Ragos, V., Galani, V. and Kyritsis, A.P. (2017) Difluoromethylornithine in cancer: new advances. *Future Oncol.*, **13**, 809–819.

18. Bassiri, H., Benavides, A., Haber, M., Gilmour, S.K., Norris, M.D. and Hogarty, M.D. (2015) Translational development of difluoromethylornithine (DFMO) for the treatment of neuroblastoma. *Transl. Pediatr.*, **4**, 226–238.

19. Pendeville, H., Carpino, N., Marine, J.C., Takahashi, Y., Muller, M., Martial, J.A. and Cleveland, J.L. (2001) The ornithine decarboxylase gene is essential for cell survival during early murine development. *Mol. Cell. Biol.*, **21**, 6549–6558.

20. Guo, Y., Cleveland, J.L. and O'Brien, T.G. (2005) Haploinsufficiency for odc modifies mouse skin tumor susceptibility. *Cancer Res.*, **65**, 1146–1149.

21. Kahana, C. (2018) The antizyme family for regulating polyamines. *J. Biol. Chem.*, **293**, 18730–18735.

22. Kurian, L., Palanimurugan, R., Godderz, D. and Dohmen, R.J. (2011) Polyamine sensing by nascent ornithine decarboxylase antizyme stimulates decoding of its mRNA. *Nature*, **477**, 490–494.

23. Fujita, K., Murakami, Y. and Hayashi, S. (1982) A macromolecular inhibitor of the antizyme to ornithine decarboxylase. *Biochem. J.*, **204**, 647–652.

24. Ray, R., Bavaria, M. and Johnson, L. (2015) Interaction of polyamines and mTOR signaling in the synthesis of antizyme (AZ). *Cell. Signal.*, **27**, 1850–1859.

25. Siedlecka, M., Szlufik, S., Grajkowska, W., Roszkowski, M. and Jozwiak, J. (2015) Erk activation as a possible mechanism of transformation of subependymal nodule into subependymal giant cell astrocytoma. *Folia Neuropathol.*, **53**, 8–14.

26. Han, S., Santos, T.M., Puga, A., Roy, J., Thiele, E.A., McCollin, M., Stemmer-Rachamimov, A. and Ramesh, V. (2004) Phosphorylation of tuberin as a novel mechanism for somatic inactivation of the tuberous sclerosis complex proteins in brain lesions. *Cancer Res.*, **64**, 812–816.

27. Mietzsch, U., McKenna, J., III, Reith, R.M., Way, S.W. and Gambello, M.J. (2013) Comparative analysis of Tsc1 and Tsc2 single and double radial glial cell mutants. *J. Comp. Neurol.*, **521**, 3817–3831.

28. Crino, P.B. (2015) mTOR signaling in epilepsy: insights from malformations of cortical development. *Cold Spring Harb. Perspect. Med.*, **5**, 1–17.

29. Nieto, M., Monuki, E.S., Tang, H., Imitola, J., Haubst, N., Khoury, S.J., Cunningham, J., Gotz, M. and Walsh, C.A. (2004) Expression of Cux-1 and Cux-2 in the subventricular zone and upper layers II-IV of the cerebral cortex. *J. Comp. Neurol.*, **479**, 168–180.

30. Murray Stewart, T., Dunston, T.T., Woster, P.M. and Casero, R.A.J. (2018) Polyamine catabolism and oxidative damage. *J. Biol. Chem.*, **293**, 18736–18745.

31. Schipper, H.M., Song, W., Tavitian, A. and Cressatti, M. (2019) The sinister face of heme oxygenase-1 in brain aging and disease. *Prog. Neurobiol.*, **172**, 40–70.

32. DiNardo, A., Kramvis, I., Cho, N., Sadowski, A., Meikle, L., Kwiatkowski, D. and Sahin, M. (2009) Tuberous sclerosis complex activity is required to control neuronal stress responses in an mTOR-dependent manner. *J. Neurosci.*, **29**, 5926–5937.

33. Reith, R.M., Way, S.W., McKenna, J., III, Haines, K. and Gambello, M.J. (2011) Loss of tuberous sclerosis complex protein tuberin causes Purkinje cell degeneration. *Neurobiol. Dis.*, **43**, 113–122.

34. Li, J., Shin, S., Sun, Y., Yoon, S.O., Li, C., Zhang, E., Yu, J., Zhang, J. and Blenis, J. (2016) mTORC1-driven tumor cells are highly sensitive to therapeutic targeting by antagonists of oxidative stress. *Cancer Res.*, **76**, 4816–4827.

35. Boer, K., Jansen, F., Nellist, M., Redeker, S., van den Ouweland, A.M., Spliet, W.G., van Nieuwenhuizen, O., Troost, D., Crino, P.B. and Aronica, E. (2008) Inflammatory process in cortical tubers and subependymal giant cell tumors of tuberous sclerosis complex. *Epilepsy Res.*, **78**, 7–21.

36. Kassai, H., Sugaya, Y., Noda, S., Nakao, K., Maeda, T., Kano, M. and Aiba, A. (2014) Selective activation of mTORC1 signaling recapitulates microcephaly, tuberous sclerosis, and neurodegenerative diseases. *Cell Rep.*, **7**, 1626–1639.

37. Zhang, B., Zou, J., Han, L., Rensing, N. and Wong, M. (2016) Microglial activation during epileptogenesis in a mouse model of tuberous sclerosis complex. *Epilepsia*, **57**, 1317–1325.

38. Cervelli, M., Angelucci, E., Germani, F., Amendola, R. and Mariottini, P. (2014) Inflammation, carcinogenesis and neurodegeneration studies in transgenic animal models for polyamine research. *Amino Acids*, **46**, 521–530.

39. Meikle, L., Talos, D.M., Onda, H., Pollizzi, K., Rotenberg, A., Sahin, M., Jensen, F.E. and Kwiatkowski, D.J. (2007) A mouse model of tuberous sclerosis: neuronal loss of Tsc1

causes dysplastic and ectopic neurons, reduced myelination, seizure activity, and limited survival. *J. Neurosci.*, **27**, 5546–5558.

40. Griffiths, P.D., Bolton, P. and Verity, C. (1998) White matter abnormalities in tuberous sclerosis complex. *Acta Radiol.*, **39**, 482–486.

41. Makki, M., Chugani, D., Janisse, J. and Chugani, H. (2007) Characteristics of abnormal diffusivity in normal-appearing white matter investigated with diffusion tensor MR imaging in tuberous sclerosis comnplex. *Am. J. Neuroradiol.*, **28**, 1662–1667.

42. Tang, Y., El-Chemaly, S., Tayeira-Dasilva, A., Goldberg, H.J., Bagwe, S., Rosas, I.O., Moss, J., Priolo, C. and Henske, E.P. (2019) Alterations in polyamine metabolism in patients with lymphangioleiomyomatosis and tuberous sclerosis complex 2-deficient cells. *Chest*, **156**, 1137–1148.

43. Bupp, C.P., Schultz, C.R., Uhl, K.L., Rajasekaran, S. and Bachmann, A.S. (2018) Novel de novo pathogenic variant in the ODC1 gene in a girl with developmental delay, alopecia, and dysmorphic features. *Am. J. Med. Genet. A*, **176**, 2548–2553.

44. Rodan, L.H., Anyane-Yeboa, K., Chong, K., Klein Wassink-Ruiter, J.S., Wilson, A., Smith, L., Kothare, S.V., Rajabi, F., Blaser, S., Ni, M. *et al.* (2018) Gain-of-function variants in the ODC1 gene cause a syndromic neurodevelopmental disorder associated with macrocephaly, alopecia, dysmorphic features, and neuroimaging abnormalities. *Am. J. Med. Genet. A*, **176**, 2554–2560.

45. Halmekyto, M., Alhonen, L., Wahlfors, J., Sinervirta, R., Eloranta, T. and Janne, J. (1991) Characterization of a transgenic mouse line over-expressing the human ornithine decarboxylase gene. *Biochem. J.*, **278**, 895–898.

46. Halonen, T., Sivenius, J., Miettinen, R., Halmekyto, M., Kauppinen, R., Sinervirta, R., Alakuijala, L., Alhonen, L., MacDonald, E. and Janne, J. (1993) Elevated seizure threshold and impaired spatial learning in transgenic mice with putrescine overproduction in the brain. *Eur. J. Neurosci.*, **5**, 1233–1239.

47. Bell, M.R., Belarde, J.A., Johnson, H.F. and Aizenman, C.D. (2011) A neuroprotective role for polyamines in a *Xenopus* tadpole model of epilepsy. *Nat. Neurosci.*, **14**, 505–512.

48. Noto, T., Hashimoto, H., Nakao, J., Kamimura, H. and Nakajima, T. (1986) Spontaneous release of gamma-aminobutyric acid formed from putrescine and its enhanced Ca2+-dependent release by high K+ stimulation in the brains of freely moving rats. *J. Neurochem.*, **46**, 1877–1880.

49. Beckonert, N.M., Opitz, T., Pitsch, J., Soares da Silva, P. and Beck, H. (2018) Polyamine modulation of anticonvulsant drug response: a potential mechanism contributing to pharmacoresistance in chronic epilepsy. *J. Neurosci.*, **38**, 5596–5605.

50. Zhou, J., Shrikhande, G., Xu, J., McKay, R.M., Burns, D.K., Johnson, J.E. and Parada, L.F. (2011) Tsc1 mutant neural stem/progenitor cells exhibit migration deficits and give rise to subependymal lesions in the lateral ventricle. *Genes Dev.*, **25**, 1595–1600.

51. Magri, L., Cambiaghi, M., Cominelli, M., Alfaro-Cervello, C., Cursi, M., Pala, M., Bulfone, A., Garcia-Verdugo, J.M., Leocani, L., Minicucci, F. *et al.* (2011) Sustained activation of mTOR pathway in emryonic neural stenm cells leads to development of tuberous sclerosis complex-associated lesions. *Cell Stem Cell*, **9**, 447–462.

52. Selamnia, M., Mayeur, C., Robert, V. and Blachier, F. (1998) Alpha-difluoromethylornithine (DFMO) as a potent arginase activity inhibitor in human colon carcinoma cells. *Biochem. Pharmacol.*, **55**, 1241–1245.

53. Origanti, S., Nowotarski, S.L., Carr, T.D., Sass-Kuhn, S., Xiao, L., Wang, J.Y. and Shantz, L.M. (2012) Ornithine decarboxylase mRNA is stabilized in an mTORC1-dependent manner in Ras-transformed cells. *Biochem. J.*, **442**, 199–207.

54. Nowotarski, S.L., Feehan, R.P., Presloid, C. and Shantz, L.M. (2018) Knockout of raptor destabilizes ornithine decarboxylase mRNA and decreases binding of HuR to the ODC transcript in cells exposed to ultraviolet-B irradiation. *Biochem. Biophys. Res. Commun.*, **505**, 1022–1026.

55. Uhlmann, E., Apicelli, A., Baldwin, R., Burke, S., Banjenaru, M., Onda, H., Kwiatkowski, D. and Gutmann, D. (2002) Heterozygosity for the tuberous sclerosis complex (TSC) gene products results in increased astrocyte numbers and decreased p27-Kip1 expression in TSC2+/- cells. *Oncogene*, **21**, 4050–4059.

56. Uhlmann, E.J., Wong, M., Baldwin, R.L., Bajenaru, M.L., Onda, H., Kwiatkowski, D.J., Yamada, K. and Gutmann, D.H. (2002) Astrocyte-specific TSC1 conditional knockout mice exhibit abnormal neuronal organization and seizures. *Ann. Neurol.*, **52**, 285–296.

57. Zou, J., Zhang, B., Gutmann, D.H. and Wong, M. (2017) Postnatal reduction of tuberous sclerosis complex 1 expression in astrocytes and neurons causes seizures in an age-dependent manner. *Epilepsia*, **58**, 2053–2063.

58. Grabole, N., Zhang, J., Aigner, S., Ruderisch, N., Costa, V., Weber, F., Theron, M., Berntenis, N., Spleiss, O., Ebeling, M. *et al.* (2016) Genomic analysis of the molecular neuropathology of tuberous sclerosis using a human stem cell model. *Genome Med.*, **8**, 94.

59. Blair, J.D., Hockemeyer, D. and Bateup, H.S. (2018) Genetically engineered human cortical spheroid models of tuberous sclerosis. *Nat. Med.*, **24**, 1568–1578.

60. Costa, V., Aigner, S., Vukcevic, M., Sauter, E., Behr, K., Ebling, M., Dunkley, T., Friedlein, A., Zoffmann, S., Meyer, C.A. *et al.* (2016) mTORC1 inhibition corrects neurodevelopmental and synaptic alterations in a human stem cell model of tuberous sclerosis. *Cell Rep.*, **15**, 86–95.

61. Sosunov, A.A., Wu, X., Weiner, H.L., Mikell, C.B., Goodman, R.R., Crino, P.D. and McKhann, G.M., 2nd (2008) Tuberous sclerosis: a primary pathology of astrocytes? *Epilepsia*, **49**, 53–62.

62. Filous, A.R. and Silver, J. (2016) Targeting astrocytes in CNS injury and disease: a translational research approach. *Prog. Neurobiol.*, **144**, 173–187.

63. Schipper, H.M., Cisse, S. and Stopa, E.G. (1995) Expression of heme oxygenase-1 in the senescent and Alzheimer-diseased brain. *Ann. Neurol.*, **37**, 758–768.

64. Schipper, H.M., Liberman, A. and Stopa, E.G. (1998) Neural heme oxygenase-1 expression in idiopathic Parkinson's disease. *Exp. Neurol.*, **150**, 60–68.

65. Mazzuferi, M., Kumar, G., van Eyll, J., Danis, B., Foerch, P. and Kaminski, R.M. (2013) Nrf2 defense pathway: experimental evidence for its protective role in epilepsy. *Ann. Neurol.*, **74**, 560–568.

66. Ha, H.C., Sirisoma, N.S., Kuppusamy, P., Zweier, J.L., Woster, P.M. and Casero, R.A.J. (1998) The natural polyamine spermine functions directly as a free radical scavenger. *Proc. Natl. Acad. Sci. U. S. A.*, **95**, 11140–11145.

67. Das, K.C. and Misra, H.P. (2004) Hydroxyl radical scavenging and singlet oxygen quenching properties of polyamines. *Mol. Cell. Biochem.*, **262**, 127–133.

68. Muller, M., Cleef, M., Rohn, G., Bonnekoh, P., Paiunen, A.E., Bernstein, H.G. and Paschen, W. (1991) Ornithine

decarboxylase in reversible cerebral ischemia: an immuno-histochemical study. *Acta Neuropathol.*, **83**, 39–45.

69. Schipper, R.G. and Verhofstad, A.A. (2002) Distribution patterns of ornithine decarboxylase in cells and tissues: facts, problems, and postulates. *J. Histochem. Cytochem.*, **50**, 1143–1160.

70. Bernstein, H.G. and Muller, M. (1999) The cellular localization of the L-ornithine decarboxylase/polyamine system in normal and diseased central nervous system. *Prog. Neurobiol.*, **57**, 485–505.

71. Grimaldi, R., Eriksson, C.G., Eneroth, P., Agnati, L.F. and Fuxe, K. (1989) Evidence for nuclear ornithine decarboxylase activity in different brain regions of the male rat. *Neurochem. Int.*, **15**, 433–438.

72. Coleman, C.S., Stanley, B.A. and Pegg, A.E. (1993) Effect of mutations at active site residues on the activity of ornithine decarboxylase and its inhibition by active site-directed irreversible inhibitors. *J. Biol. Chem.*, **268**, 24572–24579.

73. Kabra, P.M., Lee, H.K., Lubich, W.P. and Marton, L.J. (1986) Solid-phase extraction and determination of dansyl derivatives of unconjugated and acetylated polyamines by reverse-phase liquid chromatography: improved separation systems for polyamines in cerebrospinal fluid, urine and tissue. *J. Chromatogr.*, **380**, 19–32.

74. Bradford, M.M. (1976) A rapid and sensitive method for the quantitation of microgram quantities of protein utilizing the principle of protein-dye binding. *Anal. Biochem.*, **72**, 248–254.

75. Hewett, S.J., Choi, D.W. and Gutmann, D.H. (1995) Expression of neurofibromatosis 1 (NF1) gene in reactive astrocytes *in vitro*. *Neuroreport*, **6**, 1565–1568.